ISSN 0001-4338, Izvestiya, Atmospheric and Oceanic Physics, 2021, Vol. 57, No. 2, pp. 170–179. © Pleiades Publishing, Ltd., 2021.
Russian Text © The Author(s), 2021, published in Izvestiya Rossiiskoi Akademii Nauk, Fizika Atmosfery i Okeana, 2021, Vol. 57, No. 2, pp. 188–198.

Dynamics of Nonstationary Cylindrical Solitary Internal Waves

K. A. Gorshkov[a], L. A. Ostrovsky[a], and I. A. Soustova[a, *]

[a] *Institute of Applied Physics, Russian Academy of Sciences, Nizhny Novgorod, 603950 Russia*

**e-mail: soustovai@mail.ru*

Received July 7, 2020; revised October 21, 2020; accepted December 9, 2020

Abstract—An approximate analytical description of the nonstationary evolution of cylindrical nonlinear solitary waves with a complex structure is given. A modified Gardner equation with a boundary condition in the form of a "wide" soliton close to the limiting one is analyzed. The analysis shows a qualitative difference in the behavior of converging and diverging waves, as well as a difference from the quasi-stationary dynamics of cylindrical solitons.

Keywords: internal waves, solitons, kinks, cylindrical convergence, divergence

DOI: 10.1134/S0001433821020055

INTRODUCTION

As shown by satellite observations, internal gravity waves, which are observed everywhere in the World Ocean, often have curvilinear fronts [1–3]. Such a picture is typical for internal waves generated by local disturbances in shelf regions of seas and oceans. In the literature, the influence of cylindrical divergence on propagation of long weakly linear waves was studied in detail within the framework of the integrable cylindrical Korteweg–de Vries (KdV) equation [4–10]. In particular, the law describing the variation in the amplitude of the KdV cylindrical soliton $(r/r_0)^{-2/3}$, where r_0 is the initial coordinate of the soliton, was obtained in the quasi-stationary approximation and is corroborated by many numerical and laboratory experiments [6–10]. At the same time, the amplitude of observed solitary internal waves in many cases is not small, and their width considerably exceeds that predicted in the KdV model [11–14]. In this case, the Gardner equation, which contains quadratic and cubic nonlinearities and is also often used for modeling nonlinear wave processes in a stratified liquid [11–20], can serve as a good approximation. In [14, 15], the Gardner ray equation allowing one to take into account the nonunidimensionality of wavefronts of nonlinear internal waves in the ocean with variable depth and hydrology was obtained; in [16], numerically and as part of the approximate quasi-stationary theory, the influence of weak cylindrical divergence on the transformation of solitary internal waves of different types existing at different signs of nonlinearity coefficients and dispersion of the Gardner equation was studied. The very widespread two-layer fluid model is characterized by the existence of limiting amplitude solitons [17]. Solitons close to limiting (we call them large) have the form of rectilinear pulses and can be treated as composite structures formed by more elementary stationary waves—kinks (field drops). Similar solitons with a composite structure were also found in a numerical investigation of Euler equations in a smoothly stratified fluid [18]. As established in [16], the dynamics of a cylindrically diverging wide soliton in the quasi-stationary approximation qualitatively differs from the similar dynamics of a KdV soliton: first, such a soliton preserves the almost limiting amplitude, becomes narrower, and only then begins to decrease in the amplitude according to the quasi-stationary law $(r/r_0)^{-2/3}$ typical for KdV solitons and, correspondingly, to expand as $(r/r_0)^{2/3}$. At the same time, for wide solitons, an approximate approach was developed [21–24]. It presents an analytical description of the significantly nonstationary evolution of such solitary waves which are already dissimilar to solitons in shape. In addition, the shape of the initial solitary wave can be significantly distorted, up to the birth of new solitons. The main idea in this approach is the transition from the traditional description of the evolution of solitons as integral formations to the description of the evolution of kinks constituting them and nonstationary fields beyond the kinks. Using this approach allows one to study nonstationary processes appearing during the interaction of solitons [12, 21] and their propagation in media with variable parameters [22–24], when the scales of disturbing factors become comparable and even significantly less than scales of solitary waves. In particular, using this approach, parameters of solitary internal waves were successfully calculated at the so-called critical points related to the change in the sign of the quadratic nonlinearity of the Gardner equation [24, 28]. Such situations are typical, in par-

ticular, for solitary internal waves in the shelf zone of oceans and seas [25–28].

In this work, based on the abovementioned approach, the essentially nonstationary behavior of cylindrically diverging and converging localized waves in the Gardner equation is studied. For brevity, we call them quasi-solitons. Converging (focused) waves are considered not only due to nontrivial features of their evolution, but also due to the fact that such waves can be observed in a real ocean, e.g., when a diverging wave is reflected from a steep concave shore.

WIDE SOLITONS AS COMPOSITE FORMATIONS

We proceed from the Gardner equation supplemented with a summand responsible for the cylindrical geometry of the problem far from the center [16, 25, 26]:

$$\tilde{\Phi}_r + \tilde{\Phi}\left(\alpha_0 - \mu_0\tilde{\Phi}\right)\tilde{\Phi}_m + \beta\tilde{\Phi}_{mmm} = -\frac{\tilde{\Phi}}{2r}. \qquad (1)$$

According to [25, 26], the variable $\tilde{\Phi}$ in the mode approach is related to the displacement of particles at the horizon of the maximum of the corresponding mode and $T = \frac{r}{c_0} \pm t$ is time in the accompanying system of coordinates; the signs ($\pm$) relate to converging and diverging waves, respectively. For internal waves, parameters α_0, μ_0, and β and the velocity of long linear waves c_0 are determined by liquid stratification. The applicability limits of Eq. (1) were discussed, e.g., in [29].

The change of the variable $\tilde{\Phi} = \Phi\sqrt{\frac{r_0}{r}}$ reduces Eq. (1) to an equation with variable coefficients:

$$\Phi_r + \Phi\left(\alpha(r) - \mu(r)\Phi\right)\Phi_T + \beta\Phi_{TTT} = 0, \qquad (2)$$

where

$$\alpha(r) = \frac{\alpha_0}{\sqrt{r/r_0}}, \quad \mu(r) = \frac{\mu_0}{r/r_0}.$$

Gardner equation (1) with a zero right-hand side describes the evolution of solitons of internal moderate amplitude waves in a two-layer fluid well; a generalization of (1) to the case of parameters slowly varying in the horizontal direction was presented in [14, 15]. In problem (2), which is evolutionary in the variable r, growing values $r > r_0$ are in correspondence with cylindrically diverging fronts; converging fronts correspond to decreasing values $r < r_0$.

At constant coefficients α, β, and $\mu > 0$, Eq. (2) has a family of soliton solutions:

$$\phi_s = \overline{\phi} + \frac{A}{2}\left[\tanh\left((T - sr + \Delta/2)/\tau\right) - \tanh\left((T - sr - \Delta/2)/\tau\right)\right], \qquad (3a)$$

depending on an arbitrary pedestal $\overline{\phi} = \text{const}$ and dimensionless parameter $b = \Delta/\tau$. All other parameters entering into expression (3a) can be written in terms of $\overline{\phi}$ and b:

$$A = \phi_m\tanh b, \ \tau = \frac{\tau_m}{\tanh b}, \ \Delta = b\tau_m\coth b,$$
$$s = s_0 + (s - s_0)\tanh^2 b, \phi_m = (\alpha/\mu) - 2\overline{\phi}, \qquad (3b)$$
$$s_m = \left(\alpha^2/6\mu\right) + \frac{s_0}{3}, \ s_0 = \overline{\phi}\left(\alpha - \mu\overline{\phi}\right), \ \tau_m^{-1} = \phi_m\sqrt{\frac{\mu}{6\beta}}.$$

The soliton amplitude $\phi_{\max} = \max\left(\left|\phi_s - \overline{\phi}\right|\right)$ and duration T_s at the level $\frac{1}{2}\phi_{\max}$ can also be expressed in terms of b:

$$\phi_{\max} = \phi_m\left(1 - ch^{-1}b\right), \quad \cosh\left(T_s/\tau\right) = 2 + \cosh b. \qquad (3c)$$

The dimension of parameters s, s_m, and s_0 entering into (3a), (3b), and (3c) is inverse to velocity. For brevity, below we call them slownesses. Note, however, that the quantity s in physical variables (r, t) is proportional to the addition to the velocity c_0.

In addition to soliton solutions, Eq. (2) at constant parameters has a one-parameter family of solutions in the form of field drops—kinks:

$$\phi_k = \overline{\phi} + \frac{\phi_m}{2}\left[1 \pm \tanh\left((T - rs_m)/\tau_m\right)\right], \qquad (4)$$

where $\pm$ corresponds to kinks of different polarities (kinks and antikinks).

The structure and characteristics of solitons (3a) significantly depend on the magnitude of the parameter b. At $b \ll 1$, the soliton amplitude is small ($\phi_{\max} \approx \phi_m b^2$) and solution (3a)–(3c) is close to the soliton KdV solution. In the other limiting case, when $b \gg 1$, the soliton amplitude tends to the limit ($\phi_{\max} = \phi_m$) and the solitary wave acquires a rectangular shape in the form of an extended plateau with a duration $\Delta = b\tau_m$. The plateau is bounded by relatively narrow field drops close to kinks (4). In the general case, solitons (3a) can be considered composite formations formed by kinks (4) of different polarity. This property manifests itself in the most obvious way in solitons at $b \gg 1$, when, as shown in [22–24], solution (3) has the form of a superposition of kinks (4):

$$\phi_s(T - sr)_{b\gg 1} = \phi_k\left(T - T_f(r)\right) + \phi_k\left(T - T_c(r)\right) - \overline{\phi} - \phi_m = \overline{\phi} + \frac{\phi_m}{2} \times \left[\tanh\left((T - T_f(r))/\tau_m\right) - \tanh\left((T - T_c(r))/\tau_m\right)\right], \qquad (5)$$

where variations in time coordinates of the front $T_f(r)$ and drop $T_c(r)$ are determined by the equations

$$\frac{dT_f}{dr} = \frac{dT_c}{dr} = s_m - 4(s_m - s_0)\exp\left[-\frac{(T_f - T_c)}{\tau_m}\right]. \quad (6)$$

Solutions (5), (6) describe a stationary composite soliton, duration $T_f - T_c$ of which is connected with parameters of the kink $\frac{dT_{f,c}}{dr}$ by Eq. (6) which agrees with the exact relation for slowness s from (3a). Indeed, at $b \gg 1$, we obtain from (3a)

$$s = s_0 + (s_m - s_0)\tanh^2 b \approx s_m - 4(s_m - s_0) \times \exp\left[-\frac{(T_f - T_c)}{\tau_m}\right].$$

In the presence of disturbances caused by the smooth variation of parameters $\alpha(r)$ and $\mu(r)$ in (2), the evolution of the composite soliton can be described as the dynamics of kinks constituting it, in agreement with the slow variation of the field beyond the kinks. Such an approach includes as a particular case the previously considered quasi-stationary evolution of the soliton as a whole, when its spatiotemporal scales remain small when compared to the scale of disturbing factors during the propagation [16]. Let us briefly discuss this problem for wide solitons using the approach developed here. In this case, the shape of the wide soliton remains close to rectangular, its amplitude is close to limiting $\phi_m = (\alpha/\mu) - 2\bar{\phi}$, and the duration $\Delta = (T_f(r) - T_c(r))$ is determined by Eq. (6). However, it is simpler to determine the last dependence from preservation of the integral in Eq. (2): $\int_{-\infty}^{+\infty}\phi_s^2 dt = P_0 = \text{const}$ [13, 25].

Taking into account the rectangular shape of the wave and setting $\bar{\phi} = 0$, we immediately obtain $\Delta(r)\phi_m^2 = \text{const}$; for a wide cylindrical soliton, it follows that

$$\Delta(r) = \Delta(r_0)\frac{r_0}{r}. \quad (7)$$

Note that the amplitude of the cylindrical soliton for the initial variable $\tilde{\Phi}$and its inverse velocity s_m do not depend on r and are equal to $\frac{\alpha_0}{\mu_0}$ and $\frac{\alpha_0^2}{6\mu_0}$, respectively. In contrast to known results (see, e.g., [16]), relation (7) describes in an explicit form the variation in the single parameter of the composite cylindrical soliton—its width $\Delta(r)$. Note that dependence (7) also follows from the general expression for the integral presented above; the expression is valid for solitons with any $0 < b < \infty$:

$$b - \tanh b = B\alpha(r)^{-1}\mu(r)^{\frac{3}{2}}\beta^{-\frac{1}{2}} = C\frac{r_0}{r}\alpha_0^{-1}\mu_0^{\frac{3}{2}}\beta^{-\frac{1}{2}}, \quad (8)$$

where the constants B and C are determined by the condition at $r = r_0$. At $b \gg 1$, expression (8) is reduced to (7); at $b \ll 1$, (8) implies the abovementioned law of variation in the amplitude of the cylindrical KdV soliton.

CONSTRUCTION OF THE NONSTATIONARY SOLUTION

Let us turn to the main case, where the pulse loses its shape close to a stationary soliton and acquires a composite (quasi-soliton) structure consisting of a smoothly varying vertex bounded by sharp field drops (kinks) which vary in a quasi-stationary manner. According to the method of matched asymptotic expansions in the form proposed in [21–24], the solution is first constructed separately for kinks and for significantly more extended regions between them; then, these solutions are joined. Here, it is assumed that the scale of the disturbing factor (in this case, the radius r) significantly exceeds the kink width. Such an interrelation of scales allows one to consider the evolution of each kink as quasi-stationary, i.e., described according to (4), and the slow variation in the field beyond kinks is determined by Eq. (2) in the dispersion-free approximation:

$$\Phi_r + \Phi\left(\frac{\alpha_0}{\sqrt{r/r_0}} - \frac{\mu_0}{r/r_0}\Phi\right)\Phi_T = 0, \quad (9)$$

i.e., by the equation of a simple wave with variable parameters. In what follows, for simplicity, parameters α_0, μ_0, and β are set to be unity.

The solution of Eq. (9) is well-known; it is reduced to the solution of the characteristic system of equations in ordinary derivatives:

$$\frac{dT}{dr} = \Phi\left(\sqrt{r_0/r} - \frac{r_0}{r}\Phi\right), \quad \frac{d\Phi}{dr} = 0, \quad (10)$$

which determines characteristic lines in the (r,T) field; along the lines, the field $\Phi(r,T)$ is transported without any change in its magnitude.

To determine the initial and boundary conditions of (9), we use the assumption above about the quasi-stationary character of the kink evolution. This makes it possible to connect the slowly varying fields adjacent to the kink which lies on radius r at time $T_k(r)$. Let us denote this field at $T > T_k(r)$ as $\Phi_k^+(r)$ and the field at $T < T_k(r)$ as $\Phi_k^-(r)$, as is shown in Fig. 1. Here, $k = f$ for the leading kink (front) and $k = c$ for the rear kink (drop). Note that, since characteristics (10) transport disturbances from the front to the drop, the wave before the leading kink propagates independently from the field behind it, although it has an effect on this field. In particular, if this field is zero at the initial point, it remains equal to zero during the evolution.

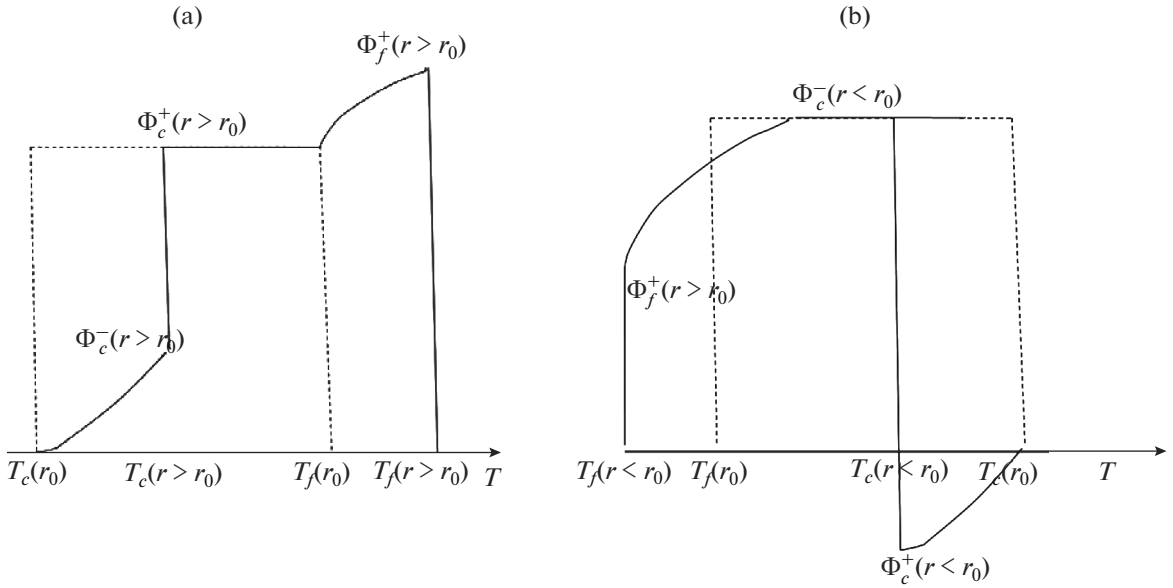

Fig. 1. Scheme of the evolution of the (a) diverging and (b) converging wide soliton (the dashed line is the soliton shape at the initial point, at $r = r_0$; the solid line is the soliton shape at (a) $r > r_0$ and (b) $r < r_0$). $T_f(r_0)$ is the instant of the front passage through the point r_0 and $T_c(r_0)$ is the instant of the drop passage through the same point. $\Phi_{f,c}^+$ are values of the field at $T > T_{f,c}$ and $\Phi_{f,c}^-$ are those at $T < T_{f,c}$ for the front and drop, respectively. Here and below, in the given frame of reference, the converging wave is displaced to the left; the diverging wave is given to the right along the T axis.

The relation between the fields directly near the kink (an analog of the boundary condition at the weakly shock wave in a compressible medium) has the form

$$\Phi_{\rm k}^+(r) = \sqrt{r/r_0} - \Phi_{\rm k}^-(r), \quad {\rm k} = f, {\rm c}. \tag{11}$$

This relation follows from the expressions for asymptotics of kink (4), which are equal to $\Phi^+ = \overline{\phi} + \phi_m$, $\Phi^- = \overline{\phi}$ for the kink and $\Phi^+ = \overline{\phi}$, $\Phi^- = \overline{\phi} + \phi_m$ for the antikink, respectively, and the elimination of $\overline{\phi}$ using the determination of ϕ_m from (3a).

Trajectories of kinks $T_k(r)$ are determined by the quasi-stationary expression for s_m following from (3a):

$$\frac{dT_k}{dr} = \frac{1}{6} + \frac{\overline{\phi}}{3}\left(\sqrt{r_0/r} - \frac{r_0}{r}\overline{\phi}\right). \tag{12}$$

The part of the slowly varying pedestal $\overline{\phi}$ in (12) can be played both by the quantity $\Phi_k^+(r)$ and by the quantity $\Phi_k^-(r)$ because, with allowance for (11), the equality of characteristic slownesses—the right-hand sides in the first equation of (10)—is valid: $\Phi_{\rm k}^+\left(\sqrt{r_0/r} - \frac{r_0}{r}\Phi_{\rm k}^+\right) = \Phi_{\rm k}^-\left(\sqrt{r_0/r} - \frac{r_0}{r}\Phi_{\rm k}^-\right)$; they, in turn, appear to be less than the quantities $\frac{dT_k}{dr}$ from (12). The last fact means that, as was mentioned above, the disturbances generated by the kink are behind it and have no effect on the field before it. Therefore, as the line of initial data for solution (9), one should take the trajectory of the kink (e.g., the front) $T_f(r)$ with the distribution of the field Φ_f^+ on it for converging fronts and Φ_f^- for diverging ones. As a result, Eq. (12) determines the slowly varying field $\Phi(r,T)$ in the region between kinks, i.e., at all $T > T_f(r)$ for converging fronts and $T < T_f(r)$ for diverging fronts, including the field near the trajectory of the next kink, at $T = T_c(r)$, which is found from Eq. (12) using the obtained solution $\Phi(T,r)$ at $T = T_c(r)$. Then, adding the field distribution directly after the drop from relation (11) to the dependence $T_c(r)$, we obtain the initial conditions for the determination of the slow field in region following the soliton drop. Thus, the construction of the general solution using the proposed algorithm consists of a consequent determination of fields $\Phi(T,r)$ and trajectories of kinks and antikinks $T_{f,c}(r)$ beginning from the region situated before the first kink and corresponding to the front.

Let us consider in more detail the situation where disturbances before the soliton at the initial point $r = r_0$ are absent and, therefore, according to what has been said, will be also absent in what follows. This makes it possible to immediately determine from (10)–(12) the magnitude of the field near the quasi-soliton front

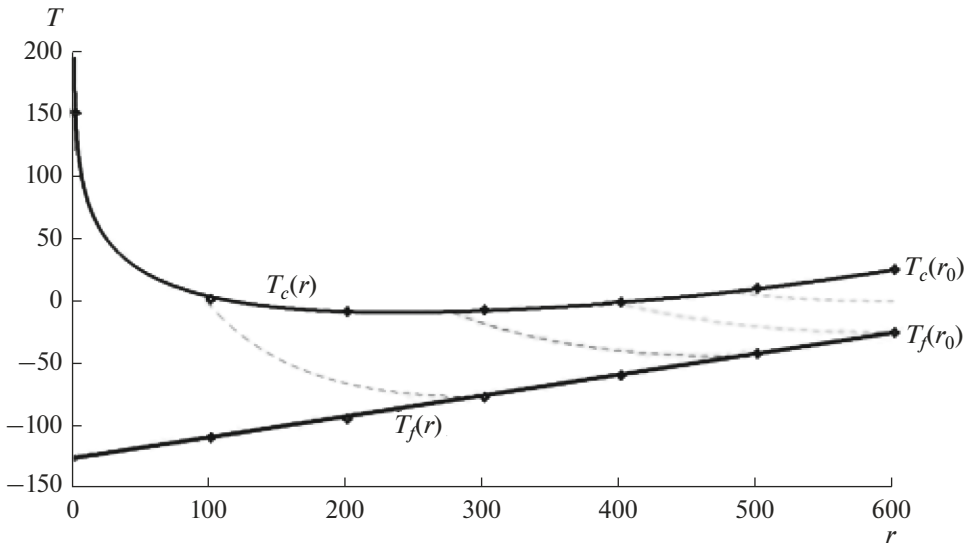

Fig. 2. Solid lines are trajectories of the front and drop of a converging soliton, dashed lines are characteristics calculated by Eqs. (10)–(12), and dots are the results of the numerical calculation of Eq. (2).

from the direction of the vertex $\Phi^+(r) = \Phi_f(r)$ and the trajectory of this front $T_f(r)$:

$$\Phi_f(r) = \sqrt{r/r_0}, \tag{12}$$

$$T_f(r) = r_0/6\left(\frac{r}{r_0} - 1\right) + T_f(r_0). \tag{13}$$

The line of initial data in (13) should be complemented by a segment

$$\Phi(r_0, t) = 1, \quad T_c(r_0) < T < T_f(r_0), \tag{14}$$

remaining from the flat top of the initial soliton at $r = r_0$ (see Fig. 1). Since any value Φ = const satisfies Eq. (9), this part remains flat with the field magnitude $\Phi(T, r) = 1$, and its evolution is reduced to a variation in its length. The constancy of this quantity allows one to determine the slownesses of boundary points of this part, $\frac{dT}{dr} = \left(\sqrt{r_0/r} - r_0/r\right)$, from the direction of the front and $\frac{dT}{dr} = \frac{1}{6} + \frac{1}{3}\left(\sqrt{r_0/r} - r_0/r\right)$ from the direction of the drop. As a result, the duration of the flat part of the top varies as

$$\Delta_{\text{fl}}(r) = \Delta(r_0) - 1/6\left|\int_{r_0}^{r}(1 - 2\sqrt{r_0/r})^2 dr'\right|. \tag{15}$$

This quantity decreases along the propagation path and disappears at a certain $r = r_*$ determined from (15) at $\Delta_{\text{fl}}(r_*) = 0$. At the same time, beginning from $r = r_0$, a part of the top with an inhomogeneous and nonstationary distribution of the field $\Phi(r, t)$ appears and expands directly after the front due to the front motion. The field is determined by the solution of Eq. (10) with conditions (13) and has the form

$$T - T_f(r_f(\Phi)) = r_0\Phi\left(2\left(\sqrt{r/r_0} - \sqrt{r_f(\Phi)/r_0}\right) - \Phi\ln\left(r/r_f(\Phi)\right)\right), \tag{16}$$

where $r_f = r_0\Phi^2$.

CONVERGING AND DIVERGING WAVES

Let us now consider examples of using the developed approximate theory and comparison with results of direct numerical modeling of the initial Eq. (2). Figure 2 shows the trajectories of the front, drop, and corresponding characteristics for a cylindrically converging quasi-soliton.

Expression (16) describes in an implicit form the field on a part of the quasi-soliton top from the front to the beginning of the flat part (until this part exists) and for the duration of the pulse from the front to the drop, when the flat part of the top disappears.

The region with the inhomogeneous and nonstationary distribution of the field appears also after the drop. This distribution is also described by expression (16), when the front trajectory $T_f(r_f(\Phi))$ is replaced by the drop trajectory $T_c(r_c(\Phi))$ and the dependence $r_f(\Phi)$ is replaced by $r_c(\Phi)$. They are found from the relations

$$\sqrt{r/r_0} - \Phi_c^-(r) = \Phi_c^+(r) = \Phi_f(r) - \Phi_c^-(r), \quad \frac{dT_c}{dr} = \frac{1}{6} + \frac{\Phi_c^\pm(r)}{3}\left(\sqrt{r_0/r} - \frac{r_0\Phi_c^\pm(r)}{r}\right). \tag{17}$$

For converging waves, it is necessary to use the dependence $r_c(\Phi) = r_c\left(\Phi_c^+\right)$; for diverging waves, $-r_c(\Phi) = r_c\left(\Phi_c^-\right)$. Note that the dependences $r_c(\Phi)$ and $T_c\left(r_c(\Phi)\right)$ are known until there exists the flat part of the top because the field near the drop from the direction of the top is constant and equal to unity (see Fig. 1), and all quantities in (17) are defined. After the disappearance of the flat part of the top, the field magnitude near the drop from the direction of the top changes. It is found from expression (16) at $T = T_c\left(r_c(\Phi)\right)$ both for converging solitary waves $\left(\Phi_c^-(r)\right)$ and for diverging $\left(\Phi_c^+(r)\right)$ ones:

$$T_c(r) - T_f\left(r_f\left(\Phi_c^\pm(r)\right)\right) = r_0\Phi_c^\pm\left(2\left(\sqrt{r/r_0} - \Phi_c^\pm\right) - \Phi_c^\pm \ln\left(r/r_f\left(\Phi_c^\pm\right)\right)\right). \quad (18)$$

Differentiating (18) with respect to r and excluding $\frac{dT_c}{dr}$ using (17), we obtain an equation for $\Phi_c^\pm$:

$$2r_0\left[6\sqrt{r/r_0} - 5\Phi_c^\pm + 12\Phi_c^\pm \ln\left(\frac{\Phi_c^\pm}{\sqrt{r/r_0}}\right)\right]\frac{d\Phi_c^\pm}{dr} = \left(1 - \frac{2\Phi_c^\pm}{\sqrt{r/r_0}^2}\right). \quad (19)$$

Therefore, the complete description of a slowly varying field is reduced to solving a single equation in ordinary derivatives (19) for the quantity $\Phi_c^\pm(r)$; its solution can be represented in a parametric form.

Going from the variables $\Phi_c^+(r)$ and r to the variables $p = \Phi_c^+/R$ and $R = \sqrt{r/r_0}$, it is easy to reduce (18) to an equation with separable variables; its solution has the form

$$R(p) = R\left(p_*\right) \times \exp\left[\int_{p_*}^{p} \frac{6 - 5p' + 12p' \ln p'}{1 - 10p' + 9(p')^2 - 12(p')^2 \ln p'} dp'\right], \quad (20)$$

where $p^* = \sqrt{r_0/r_*}$, $p_* \le p \le +\infty$, $p_* > 1$ for converging fronts and $0 \le p \le p_*$, $p_* < 1$ for diverging fronts.

The corresponding dependences for the pulse drop, $\Phi_c^\pm$ and T_c, also can be expressed in terms of p in a parametric form:

$$\Phi_c^+(p) = pR(p),\ \Phi_c^-(p) = R(p)(1-p),\ T_c(R) = T(r_0) - r_0\left[1/6 - R^2p^2\left[\ln p^2 + 2/p - 11/6\right]\right]. \quad (21)$$

Keeping in mind that $R(p)$ is known as a function of p, we obtain for any pair $(\Phi_c^\pm(p),\ R(p))$ and $(T_c(p),\ R(p))$ a parametric dependence on R and, consequently, on r. Finally, we present an expression for the field distribution after the drop in a parametric form:

$$\Phi(p) = R(p)(1-p),\ T(p,r) - T_c(p) = 2r_0(1-p)R(p)\left(\sqrt{r/r_0} - R(p)\right) - R(p)^2(1-p)^2 \ln\left[r/r_0\, R(p)^2\right]. \quad (22)$$

The domain of applicability of the obtained solution is, generally speaking, restricted with respect to r and T because the slowness of the evolution of the field $\Phi(r,T)$ can be broken by the appearance of singularities caused by the intersection of characteristics of (16) and leading to the formation of singularities in the form of fragments with infinite steepness and subsequent nonuniqueness of the field (which is typical for simple waves). Differentiating expression (16) with respect to Φ, we obtain the condition for the appearance of these singularities $\left(\frac{dT}{d\Phi} = 0\right)$ in the form of the transcendent equation

$$6y - 5 - 12\ln y = 0,\quad y = \sqrt{r/r_0}/\Phi, \quad (23)$$

having two real roots greater than unity: $y_1 = 1.2$ and $y_2 = 3.09$. Since the field of the quasi-soliton top is formed by disturbances transported along characteristics from the front to the drop, the quantity $y = \Phi_f/\Phi(r,T)$ for converging waves is always less than unity. Therefore, singularities do not appear in the distribution between kinks, although they are possible behind the quasi-soliton (see Fig. 3). In addition, since characteristics of (16) diverge, the field between kinks monotonically increases from the front to the drop. In this process, the time interval between the drop and the front also monotonically increases:

$$\Delta(r) = \Delta(r_0) + 1/3\int_{r_0}^{r} \Phi_c^-(r')\left(\sqrt{r/r_0} - \Phi_c^-(r')\right)\frac{r'}{r_0}dr'. \quad (24)$$

The general picture of the evolution of a converging soliton is shown in Figs. 2 and 3. The soliton front moves with a constant velocity to the point $T_f(r \to 0) = T_f(r_0) + r_0/6$, and the quasi-soliton drop moving first in the same direction as the front decelerates and stops at $r \sim 200$; then it begins to move in the opposite direction with an increasing velocity $\frac{dTc}{dr} \sim p^2 \sim r_0/r$. The characteristic scale of the field drop τ_m for the front turns out to be constant; for the drop, it tends to zero as $p \sim \sqrt{r/r_0}$. Finally, we note that the field drop at the quasi-soliton front in the initial field variables $\tilde{\Phi}(r,t)$ remains constant and equal to unity and the field at the drop increases as $\sqrt{r_0/r}$ (Fig. 3). It is

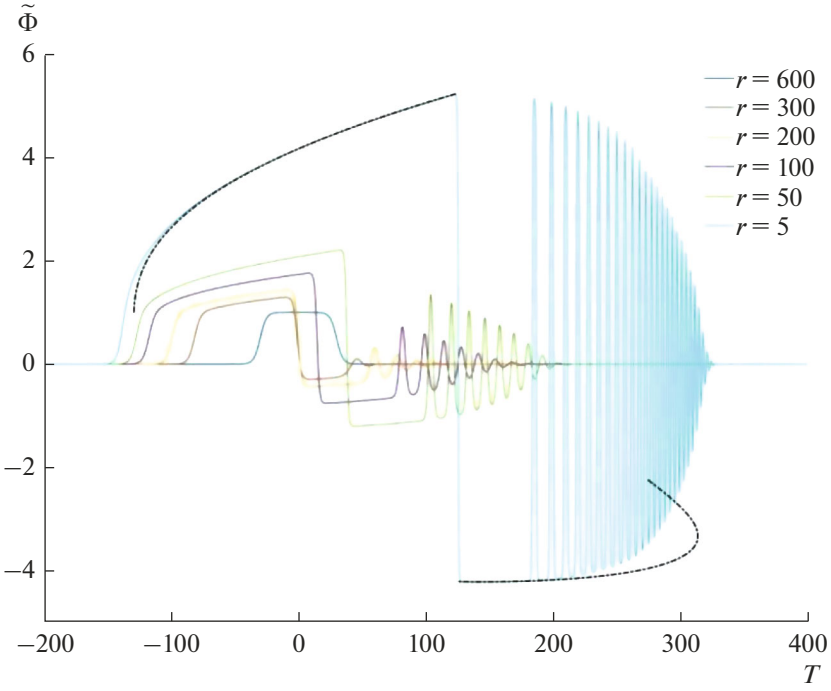

Fig. 3. Evolution of a cylindrically converging quasi-soliton with an initial duration $\Delta(r_0) = 60$ at different values of r ($r = r_0 = 600$, $r = 300$, 200, 100, 50, and 5). The dotted-and-dashed line corresponds to calculations by the approximate model and the solid lines are the numerical calculation of Eq. (2).

remarkable that, even at $r = 5$, when the scale of the field drop at the front ($6\sqrt{6}$) already exceeds the distance from the center, the prevailing part of the pulse (a considerable part of the top and the drop) is well described by the approximate theory. Since the process of field transformation goes in the direction from the front to the drop, relatively great differences at $r = 5$ take place only near the front; in particular, its position $T_f(r = 5) \cong -125$ is greater than the numerical value approximately by 20 units of T. This is caused by the action of dispersion, leading to spreading both of the front itself and of the top part, where nonlinear effects strongly steepen the field distribution (see Fig. 3). Finally, let us note that the approximate approach correctly describes the magnitude and distribution of the field on an interval of about 50 units of T in the region behind the drop up to the point $r = 1$. From the other side of this almost flat part at $r \approx 300$, a packet of oscillations appears, growing in amplitude and forming due to the upset of the slowly varying field after the quasi-soliton drop. With an increase in r, leading oscillations are transformed into a sequence of solitons with an amplitude close to limiting, i.e., approximately equal to the field jump at the drop.

For cylindrically diverging waves ($r > r_0$), the field drop on the front increases with propagation ($\Phi_f(r) = \sqrt{r/r_0}$); therefore, the field magnitude at any point of the top is less than the field magnitude on the front $(y > 1)$, and the formation of a singularity in the form of a field region with a large gradient turns out to be possible inside the quasi-soliton. In the case of the appearance of such singularity, dispersion effects lead to the appearance of oscillations, the subsequent growth of which leads to the decay of the initial soliton into a sequence of shorter solitary waves. The regular (without singularities) evolution is implemented only for relatively short quasi-solitons. The initial duration of the soliton $\Delta_{cr}(r_0)$, before which the regular evolution of the solitary wave is implemented, is found from the condition for the coincidence of coordinate r_{cr}, at which the singularity is formed, and the coordinate r_*, at which the flat part of the top disappears. Since the field value at the point of the coincidence is equal to unity, we obtain from (18) the value $r_{cr} = y_1^2 r_0 \approx 1.44 r_0$; from condition (15) $\Delta_{fl}(r_{cr}, r_0, \Delta(r_0)) = 0$, we have

$$\Delta_{cr},(r_0) = \frac{r_0}{6}\left(y_1^2 - 8y_1 + 8\ln y_1\right) \approx 0.07 r_0. \qquad (25)$$

When the evolution is regular, the pulse is monotonically compressed:

$$\Delta(r) = \Delta(r_0) - 1/3\int_{r_0}^{r} \Phi_c^+(r')\left(\sqrt{r/r_0} - \Phi_c^+(r')\right)\frac{r'}{r_0}dr', \qquad (26)$$

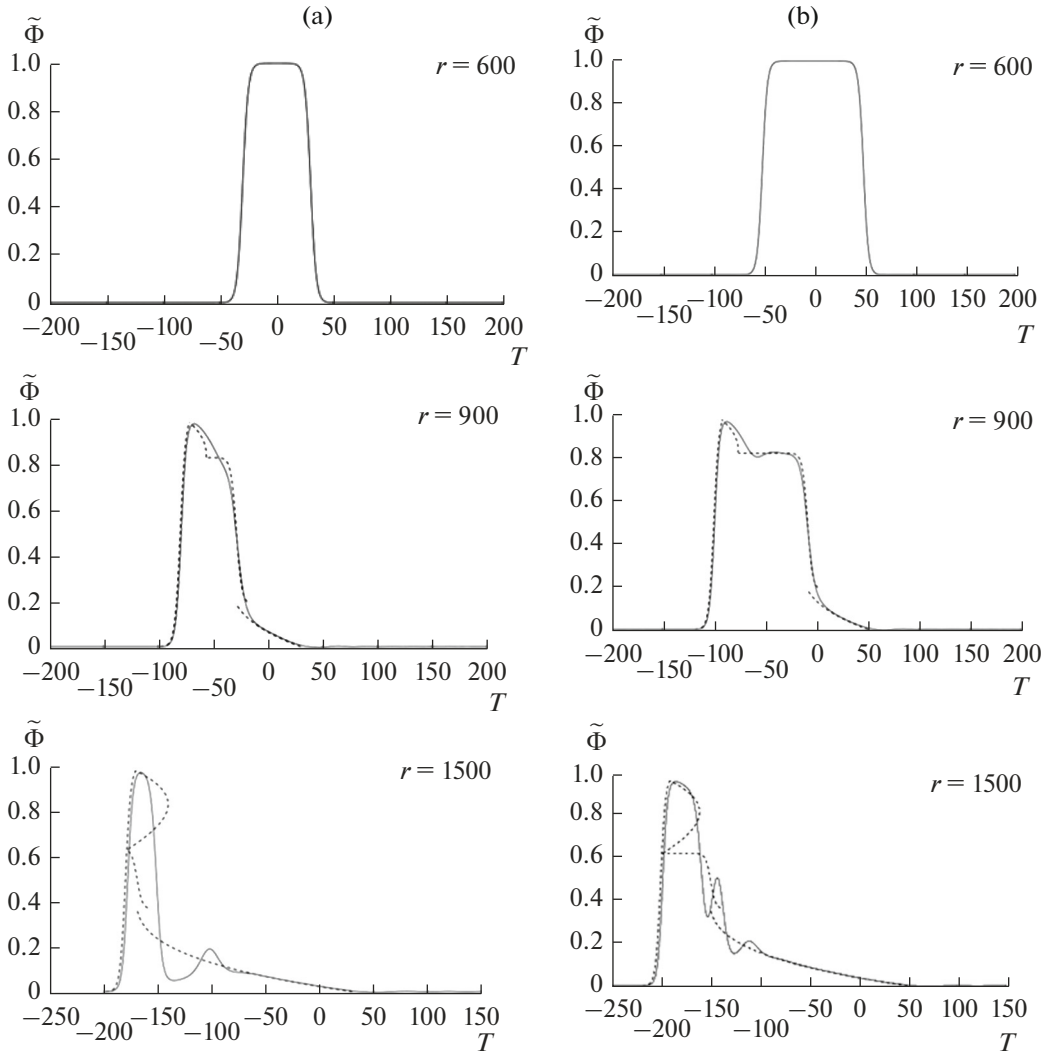

Fig. 4. (a) Evolution of a narrow $(\Delta(r_0) = 60)$ diverging composite quasi-soliton at different radii r ($r = r_0 = 600$, $r = 900$, and $r = 1500$). (b) Same for a wide soliton ($\Delta(r_0) = 100$). The solid lines are the numerical calculation of Eq. (2). The dashed lines correspond to calculations by the approximate model.

up to the formation of a short solitary wave, the further evolution of which occurs according to a scenario close to the evolution of the KdV soliton. In spite of the monotonic variation in $\Delta(r)$, the field distribution on the quasi-soliton top varies nonmonotonically: the ratio $\frac{\Phi_f}{\Phi_c^+}$ of the fields at the front and drop increases until there is a flat part of the top, and it decreases after the disappearance of the flat part; at the same time, the ratio remains greater than unity. The field after the drop with the same polarity as the quasi-soliton itself varies in a similar manner: the field amplitude first increases and begins to decrease after the disappearance of the flat part of the top (Fig. 4a). These features of the evolution of a diverging quasi-soliton are also traced for sufficiently narrow solitons considered in [16].

For a decaying wide quasi-soliton, at $\Delta(r_0) > \Delta_{cr}$, a similar process leads to the formation of new pulses at the drop. At the beginning, the first of them has a scale depending only on r_{cr}. At a later stage, however, the compression rate of this pulse is determined to a considerable extent by the quantity $\Delta(r_0)$. Since the number of shorter solitary waves appearing after the leading pulse increases with an increase in $\Delta(r_0)$, the distance at which these solitary waves detach from the leader also increases. The abovementioned effects can be seen by comparing the evolution of diverging quasi-solitons with different $\Delta(r_0)$ in Figs. 4a and 4b. Note that the approximate theory in this case well describes the whole process only up to relatively small distances, $r \simeq 1000$, although it also correctly determines the pulse position and amplitude at later stages.

Finally, note that qualitative differences in the behavior of converging and diverging wide pulses are caused by the different relationship of characteristic slownesses of top points $\frac{dT}{dr}$ and slowness of its front $\frac{dT_f}{dr}$. In converging waves, the quantity $\frac{dT}{dr}$ for any points of the top has the opposite sign with respect to $\frac{dT_f}{dr}$; therefore, the disturbances are drifted in the direction from the front to the drop at any place of the top and no singularities appear in the field distribution on the quasi-soliton top. For diverging waves, the characteristic slowness is positive at any point of the top; i.e., these points move in the same direction as the front. The slowness of each point of the top increases from zero near the front to a value exceeding the front slowness by half. At a sufficient pulse duration, disturbances from the front do not reach the drop and are accumulated, which just leads to the formation of field singularities.

CONCLUSIONS

This analysis allows one to describe the evolution of localized nonlinear cylindrical waves in the modified Gardner equation beyond the quasi-stationary situation. The initial condition corresponds here to the wide soliton; however, in the process of evolution, the pulse becomes significantly nonstationary and its approximate description is achieved by the matching of quasi-stationary kinks with a weakly dispersive field inside and outside the pulse (quasi-soliton).

For cylindrically converging solitary waves, their evolution, as in the quasi-stationary case, occurs with an increase in their duration (this trend is clear even from the condition of energy conservation). At the same time, however, their shape greatly differs from the rectangular shape and the difference in field drops and velocities of the front and drop are so great that do not allow one to characterize the process as quasi-stationary. In the case of cylindrically diverging solitons, the nonstationarity of the process is pronounced to a lesser extent when compared to the case of a converging wave. In particular, the difference between magnitudes of fields and front and drop velocities does not exceed 1.2. As expected, the duration of the solitary wave decreases both in the nonstationary and in the quasi-stationary cases; however, the regular character of the evolution turns out to be possible only for sufficiently short initial solitons. For solitary waves with a long duration, a singularity appears on their top. The singularity generates field oscillations, the growth of which, in turn, leads to the soliton decay into relatively short solitary waves. Our approach made it possible to determine, for the initial solitary wave, the critical value of the duration $\Delta = \Delta_{cr}$ beginning from which it decays: $\Delta_{cr}(r_0) \approx 0.07r_0$ (see (22)). The corresponding critical width of the soliton $L_{cr} = \frac{\Delta_{cr}}{s_m} \approx 0.42r_0$.

As for internal waves observed in the ocean, we here note that, first, as mentioned in the Introduction, wide (as compared to KdV solitons) solitary waves and their groups are observed everywhere in the ocean (see also the survey [30]) and, second, such waves not always propagate as stationary or quasi-stationary formations (e.g., [31]). In particular, the estimate above for the conditions of the transition from the quasi-stationary regime to the significantly nonstationary regime and the description of the latter for waves with curvilinear fronts can be useful for interpreting oceanic observations. A more detailed application of the theory to specific oceanic situations should be a subject of an individual investigation.

FUNDING

This work was carried out within the scope of the state contract for the Institute of Applied Physics, Russian Academy of Sciences, research and development theme no. 0035-2019-0007, and supported in part by the Russian Foundation for Basic Research, project nos. 18-05-00292 and 20-05-00776.

REFERENCES

1. C. R. Jason, J. C. DaSilva, G. A. Jeans, W. Alpers, and M. J. Caruso, "Nonlinear internal waves in synthetic aperture radar imagery," Oceanography **26**, 68–79 (2013).
2. R. A. Kropfli, L. A. Ostrovsky, T. P. Stanton, E. A. Skirta, A. N. Keane, and V. Irisov, "Relationships between strong internal waves in the coastal zone and their radar and radiometric signatures," J. Geophys. Res. **104** (C2), 3133–3148 (1999).
3. D. M. Farmer and L. Armi, "The flow of Atlantic water through the Strait of Gibraltar," Prog. Oceanogr. **21**, 1–105 (1988).
4. S. Maxon and J. Viecelli, "Cylindrical solitons," Phys. Fluids **17**, 1614–1616 (1974).
5. R. S. Johnson, "Water waves and Korteweg–de Vries equations," J. Fluid Mech. **97**, 701–719 (1980).
6. A. A. Dorfman, E. N. Pelinovskii, and Yu. A. Stepanyants, "Finite-amplitude cylindrical and spherical waves in weakly dispersive media," Sov. Phys. J. Appl. Mech. Tech. Phys., No. 2, 206–211 (1981).
7. Yu. A. Stepanyants, "Experimental investigation of cylindrically diverging solitons in an electric lattice," Wave Motion, No. **3**, 335–341 (1981).
8. P. D. Weidman and R. Zakhem, "Cylindrical solitary waves," J. Fluid Mech. **191**, 557–573 (1988).
9. R. S. Johnson, "Ring waves on the surface of shear flows: A linear and nonlinear theory," J. Fluid Mech. **215**, 145–160 (1990).
10. Yu. A. Stepanyants, "On the attenuation of internal solitary waves due to cylindrical divergence," Izv. Akad.

Nauk SSSR: Fiz. Atmos. Okeana **17** (8), 886–888 (1981).

11. T. R. Stanton and L. A. Ostrovsky, "Observations of highly nonlinear internal solitons over the continental shelf," Geophys. Res. Lett. **25** (14), 2695–2698 (1998).
12. K. A. Gorshkov, L. A. Ostrovsky, I. A. Soustova, and V. G. Irisov, "Perturbation theory for kinks and application for multisoliton interactions in hydrodynamics," Phys. Rev. E **69**, 1–10 (2004).
13. R. Grimshaw, E. Pelinovsky, and T. Talipova, "Solitary wave transformation in a medium with sign-variable quadratic nonlinearity and cubic nonlinearity," Phys. D (Amsterdam, Neth.) **132**, 40–62 (1999).
14. R. Grimshaw, E. Pelinovsky, and T. Talipova, "Modelling internal solitary waves in the coastal ocean," Surv. Geophys. **28**, 273–287 (2007).
15. O. Nakoulima, N. Zahybo, E. Pelynovsky, T. Talipova, A. Slunyaev, and A. Kurkin, "Analytical and numerical studies of the variable-coefficient Gardner equation," Appl. Math. Comput. **152**, 449–471 (2004).
16. O. E. Polukhina and N. M. Samarina, "Cylindrical divergence of solitary internal waves in the context of the generalized Gardner equation," Izv., Atmos. Ocean. Phys. **43** (6), 755–761 (2007).
17. C. J. Amick and R. E. L. Turner, "A global theory of internal solitary in two-fluid system," Trans. Am. Math. Soc. **298**, 431–484 (1986).
18. V. I. Vlasenko, P. Brandt, and A. Rubino, "On the structure of large-amplitude internal solitary waves," J. Phys. Oceanogr. **30**, 2172–2185 (2000).
19. K. R. Khusnutdinova and X. Zhang, "Long ring waves in stratified fluid over a shear flow," J. Fluid Mech. **79**, 27–44 (2016).
20. K. R. Khusnutdinova and X. Zhang, "Nonlinear ring waves in two-layer fluid," Phys. D (Amsterdam, Neth.) **333**, 208–220 (2016).
21. K. A. Gorshkov and I. A. Soustova, "Interaction of solitons as compound structures in the Gardner model," Radiophys. Quantum Electron. **44** (5), 465–476 (2001).
22. K. A. Gorshkov, I. A. Soustova, A. V. Ermoshkin, and N. V. Zaitseva, "Evolution of the compound Gardner-equation soliton in the media with variable parameters," Radiophys. Quantum Electron. **55** (5), 344–355 (2012).
23. K. A. Gorshkov, I. A. Soustova, A. V. Ermoshkin, and N. V. Zaitseva, "Approximate description of the quasistationary evolution of nearly limiting internal solitary waves using the Gardner equation with variable coefficients," Fundam. Prikl. Gidrofiz. **6** (3), 54–62 (2013).
24. K. A. Gorshkov, I. A. Soustova, and A. V. Ermoshkin, "Field structure of a quasisoliton approaching the critical point," Radiophys. Quantum Electron. **58** (10), 738–744 (2016).
25. R. Grimshaw, E. Pelinovsky, T. Talipova, and A. Kurkin, "Simulation of the transformation of internal solitary waves on oceanic shelves," J. Physic. Oceanogr. **34**, 2774–2791 (2004).
26. P. Holloway, E. Pelinovsky, and T. Talipova, "A generalized Korteweg–de Vries model of internal tide transformation in the coastal zone," J. Geophys. Res. **104** (C8), 18333–18350 (1999).
27. A. N. Serebryanyi, "Manifestation of soliton properties in internal waves on the shelf," Izv. Ross. Akad. Nauk: Fiz. Atmos. Okeana **29** (2), 244–252 (1993).
28. K. D. Sabinin and A. N. Serebryanyi, ""Hot spots" in the field of internal waves in the ocean," Acoust. Phys. **53** (3), 357–380 (2007).
29. R. Grimshaw, "Initial conditions for the cylindrical Korteweg–de Vries equation," Stud. Appl. Math. **143** (2), 176–191 (2019).
30. J. R. Apel, L. A. Ostrovsky, Yu. A. Stepanyants, and J. F. Lynch, "Internal solitons in the ocean and their effect on underwater sound," J. Acoust. Soc. Am., No. 2, 695–722 (2007).
31. J. N. Mou, D. M. Farmer, W. D. Smyth, L. Armi, and S. Vagley, "Structure and generation of turbulence at interfaces strained by internal solitary waves propagating shoreward over the continental shelf," J. Phys. Oceanogr. **33**, 2093–2112 (2003).

Translated by A. Nikolskii